Raman Spectroscopy

Deutsche Ausgabe: DOI: 10.1002/ange.201605776
Internationale Ausgabe: DOI: 10.1002/anie.201605776

Metal Nanoparticle-Catalyzed Reduction Using Borohydride in Aqueous Media: A Kinetic Analysis of the Surface Reaction by Microfluidic SERS

Wei Xie[+], Roland Grzeschik[+], and Sebastian Schlücker**

Abstract: *Hydrides are widely used in reduction reactions. In protic solvents, their hydrolysis generates molecular hydrogen as a second reducing agent. The competition between these two parallel reduction pathways has been overlooked so far since both typically yield the same product. We investigated the platinum-catalyzed reduction of 4-nitrothiophenol to 4-aminothiophenol in aqueous sodium borohydride solution as a prominent model reaction, by using label-free SERS monitoring in a microfluidic reactor. Kinetic analysis revealed a strong pH dependence. Surprisingly, only at pH > 13 the reduction is driven exclusively by sodium borohydride. This study demonstrates the potential of microfluidics-based kinetic SERS monitoring of heterogeneous catalysis in colloidal suspension.*

Sodium borohydride is one of the most widely used reducing agents in chemical synthesis.[1] This reducer is stable even at 400 °C,[2] but undergoes hydrolysis in protic solutions and generates molecular hydrogen [Eq. (1)].[3]

$$NaBH_4 + 4\,H_2O \rightarrow NaB(OH)_4 + 4\,H_2 \quad (1)$$

Quantitative studies with borohydride in aqueous solution are difficult to perform because of this instability. Furthermore, molecular hydrogen itself is also a strong reducer and therefore a competitor of hydride during the reaction.[4] This is often overlooked since the reduction product for both hydride- and H_2-driven reductions is generally the same. However, for understanding the underlying reaction mechanisms, it is mandatory to differentiate between the two competing reductions.

A prominent example for a reduction reaction in aqueous borohydride solution is the conversion of 4-nitrothiophenol (4-NTP) to 4-aminothiophenol (4-ATP), which is catalyzed by platinum.[5] In this reaction, the 4-NTP starting molecules are coated on the surface of a bifunctional substrate with both plasmonic and catalytic activity. The catalytic process occurs in the localized surface plasmon resonance (LSPR) field of the bifunctional nanostructure and surface-enhanced Raman scattering (SERS) of the adsorbed molecules is excited.[6] SERS is ideally suited for monitoring molecular changes at the metal/solution interface because of its molecular specificity in combination with high sensitivity and surface selectivity.[7] In the past few years, the reduction of 4-ATP to 4-NTP has been frequently investigated by using SERS on bifunctional substrates with different metal catalysts.[8] So far, all of them have assumed explicitly or implicitly that hydride is the actual reducing agent in aqueous borohydride solution, that is, the role of molecular hydrogen due to the hydrolysis in (1) has been overlooked. The present study was therefore undertaken for differentiating between hydride- and H_2-based reduction of 4-NTP in aqueous sodium borohydride solution. This competition has been overlooked so far since the reaction product (4-ATP) is the same in both cases.[9]

Scheme 1 summarizes the central mechanistic findings on the reaction derived from our kinetic analysis. Both hydride and molecular hydrogen lead to the formation of surface-adsorbed atomic hydrogen (Pt–H), which reacts with adsorbed 4-NTP via a Langmuir–Hinshelwood mechanism to 4-ATP.

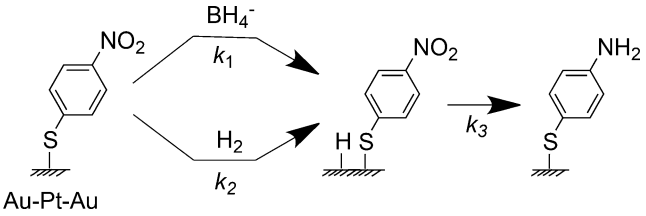

Scheme 1. Reaction Scheme showing the reduction of 4-nitrothiophenol (4-NTP) to 4-aminothiophenol (4-ATP) (with rate constant k_3) by adsorbed atomic hydrogen formed on Au-Pt-Au surface using borohydride (with rate constant k_1) and molecular hydrogen (with rate constant k_2), respectively.

Bifunctional Au-Pt-Au hybrid NPs are used as both metal catalysts and plasmonically active SERS substrates. In order to eliminate severe complications associated with standard SERS cuvette experiments, this fast (few seconds) Pt-catalyzed reduction is monitored in a custom-made microfluidic reactor, which provides 1) fast mixing of the reactants, 2) high temporal resolution (milliseconds), and 3) eliminates unwanted side reactions caused by continuous laser illumination. The kinetic analysis of time-resolved SERS spectra acquired at different pH values and temperatures allows us to disentangle hydride from H_2 reduction chemistry.

[*] Dr. W. Xie,[+] R. Grzeschik,[+] Prof. S. Schlücker
Department of Chemistry and
Center for Nanointegration Duisburg-Essen
University of Duisburg-Essen, Universitätsstr. 5
45141 Essen (Germany)
E-mail: wei.xie@uni-due.de
sebastian.schluecker@uni-due.de

[+] These authors contributed equally to this work.

Supporting information and the ORCID identification number(s) for the author(s) of this article can be found under http://dx.doi.org/10.1002/anie.201605776.

The bifunctional NPs employed in this study have a Au core, a Pt shell, and many small Au protuberance particles on the Pt shell.[5] The plasmonic coupling between the Au core and the small Au particles on the very thin Pt shell (ca. 3 nm here vs. 10 nm in Ref. [5]) enables SERS enhancement of the molecules involved in the catalytic reactions (see Figure S1 in the Supporting Information). Control experiments shown in Figure S2 confirm the role of Pt as the catalyst of the reduction from 4-NTP to 4-ATP in aqueous sodium borohydride solution. The 4-NTP-coated NP suspension is mixed with sodium borohydride solution in a temperature-controlled microfluidic mixer with 30 alternatingly combined channels (Figure 1 and Figure S3) for complete mixing within 0.1 s (see Figure S4). SERS signals from the mixture are recorded from the meander-shaped reaction channel.

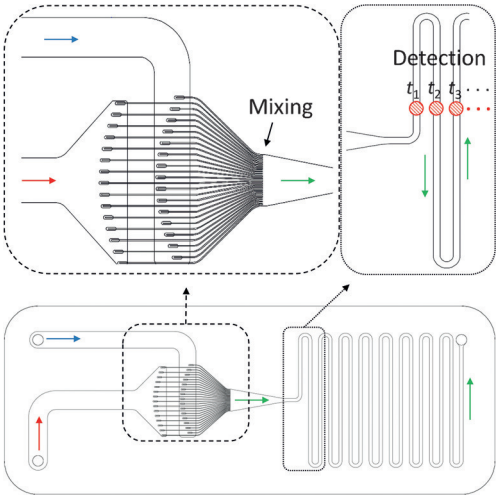

Figure 1. The microfluidic reactor chip used for label-free SERS monitoring of the reduction of 4-NTP on Au-Pt-Au bifunctional NPs in aqueous borohydride solutions. The reducing agent and the colloidal catalyst are injected into the reactor, divided into 30 channels and then recombined alternatingly for fast mixing. Time-resolved SERS spectra are recorded at different positions along the meander-shaped flow channel (top right). The red points are shown as examples for the SERS detection at different reaction times.

In conventional SERS experiments employing cuvettes, continuous laser illumination induces the photocatalytic side reaction from 4-NTP or 4-ATP to 4,4′-dimercaptoazobenzene (4,4′-DMAB).[10] Here, we eliminate this unwanted photocatalytic side reaction (red spectrum in Figure 2a) by using a microfluidic channel with a continuous flow which significantly reduces the laser illumination time for the same sample volume. When the syringe pump is switched on, the bifunctional NPs flow fast through the laser focus (ca. 1 μm) and we only detect SERS from 4-NTP (blue spectrum in Figure 2a), but not from 4,4′-DMAB. Therefore, this microfluidic SERS detection scheme allows us to directly probe reagent-induced reductions without interference from photoinduced reduction chemistry.

Furthermore, the microfluidic approach also provided the necessary time resolution for kinetic monitoring of this fast Pt-catalyzed reduction reaction. The time intervals can be

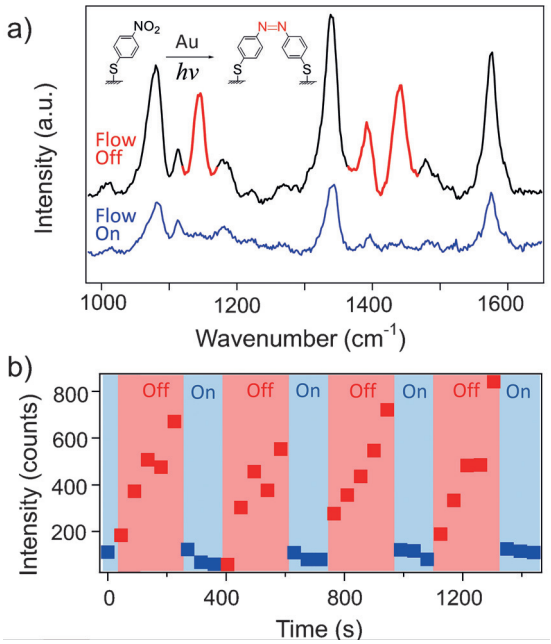

Figure 2. a) Comparison of SERS spectra from 4-NTP adsorbed on Au-Pt-Au NPs when the flow in the microfluidic channel is switched off (plasmon-induced photocatalytic side reduction from 4-NTP to 4,4′-DMAB) and on (no side reaction is detected). b) SERS intensity of the photoproduct 4,4′-DMAB (peak at 1437 cm^{-1}) for several on-off cycles.

easily increased or decreased by recording SERS spectra at different positions on the channel of the microfluidic reactor or by changing the flow rate.[11] This is not possible in static experiments employing cuvettes or capillaries since the mixing of the reactants is not fast enough and the acquisition time for each Raman/SERS spectrum is significantly longer than the half-time of the reaction.

Figure 3a shows a false color-coded intensity map of the kinetic SERS data recorded from the microfluidic reactor. The reaction time is determined only by the detection distance and the sample flow rate. Thus, one can measure as long as possible at a defined position/reaction time to improve the spectral quality. This is not possible in conventional cuvette experiments. The corresponding SERS spectra in Figure 3b and Figure S5 (detection at longer reaction times) do not contain any detectable contribution of 4,4′-DMAB from the unwanted photocatalytic side reactions. Quantitative information on the relative contributions of the 4-ATP starting material is obtained by comparing the peak areas of the phenyl ring vibrations of 4-NTP and 4-ATP at 1569 and 1591 cm^{-1}, respectively. This requires correction for their different Raman scattering cross sections/SERS intensities as determined under otherwise identical experimental conditions (see Figure S6). Figure 3c shows the determination of the rate constants at temperatures ranging from 5 to 50 °C. The reduction at 50 °C is finished after about 1 s (rate constant 4.72 s^{-1}). A time increment of 25 ms for SERS monitoring was chosen. The activation energy of this first-order reaction is (56.1 ± 3.45) kJ mol^{-1} (see Figure S7).

Since the rate constant of the hydrolysis of sodium borohydride in aqueous solution is pH-dependent,[12] we

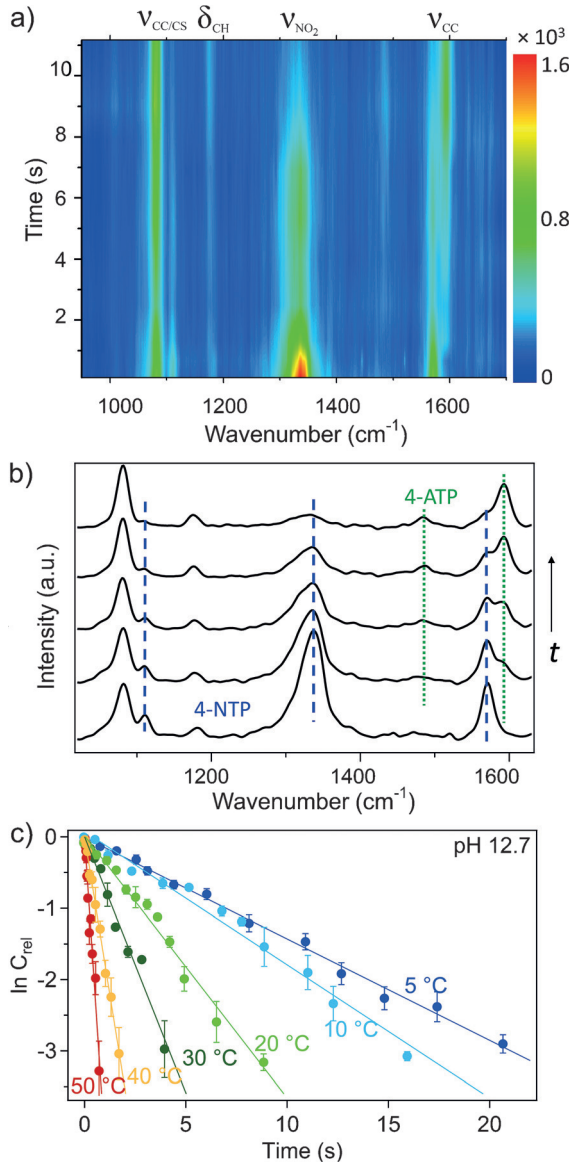

Figure 3. a) SERS false color-coded intensity map for the catalytic reduction of 4-NTP on bifunctional Au-Pt-Au NPs in aqueous sodium borohydride solution at 10 °C. The educt 4-NTP is directly converted to the product 4-ATP. No contributions from the unwanted photocatalytic side product 4,4′-DMAB are observed. b) SERS spectra recorded at different reaction times: 0.66, 1.31, 5.31, 7.91, and 11.17 s (from bottom to top). c) Determination of the rate constants (first-order kinetics) for the reduction of 4-NTP at different reaction temperatures. C_{rel} is the relative contribution of the educt 4-NTP.

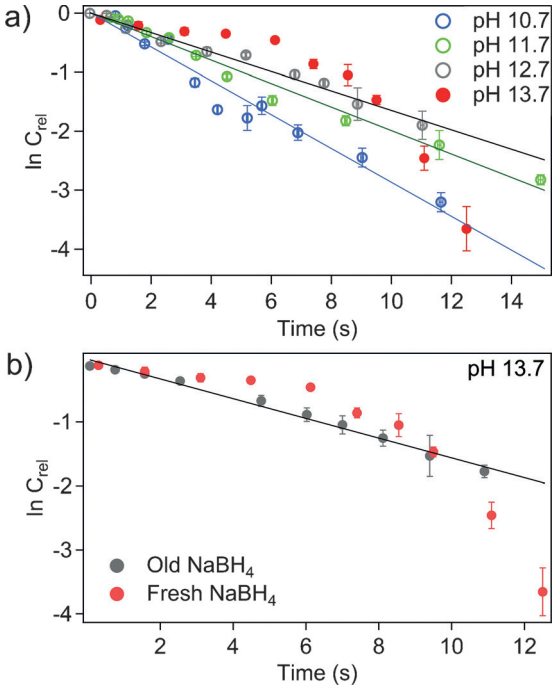

Figure 4. a) Kinetic SERS monitoring of the catalytic reduction of 4-NTP in aqueous sodium borohydride solution at different pH values (10 °C). The reaction follows first-order kinetics up to pH 13.7. b) Comparison of the reaction kinetics by using freshly prepared (red) and aged (gray) sodium borohydride solutions, respectively, at pH 13.7. The reduction using aged borohydride solution follows first-order kinetics due to the presence of H_2.

monitored the catalytic reactions at different pH values (Figure 4a). Interestingly, the reaction shows a different reaction order (zero-order) at very basic conditions (above pH 13) under which H_2 production does not occur.

The pH-dependent half-life times ($t_{1/2}$) for the hydrolysis of sodium borohydride in water are listed in Table S1. Below pH 9 at room temperature, $t_{1/2}$ is smaller than 20 seconds. We therefore performed pH-dependent SERS under basic conditions at 10 °C to slow down the hydrolysis process for kinetic SERS monitoring. Figure 4a shows that the reduction of 4-NTP follows first-order kinetics until pH 13. This result is consistent with previous studies without pH control.[8a,13] At pH > 13, however, sodium borohydride is stable in water and molecular hydrogen does not form. Therefore, the observed zero-order reduction is exclusively caused by hydride [Eq. (2)].

$$4\,R{-}NO_2 + 3\,NaBH_4 + 4\,H_2O \rightarrow 4\,R{-}NH_2 + 3\,NaB(OH)_4 \qquad (2)$$

In contrast, the reduction of 4-NTP by H_2 gas has been reported to follow first-order kinetics.[9] Thus it is very likely that at pH < 13 the reduction proceeds through H_2 (first-order kinetics) because H_2 is generated in aqueous solution by hydrolysis as shown in Equation (1) [Eq. (3)].

$$R{-}NO_2 + 3\,H_2 \rightarrow R{-}NH_2 + 2\,H_2O \qquad (3)$$

In order to confirm this hypothesis, reactions with fresh and old sodium borohydride solutions are compared (Figure 4b). Sodium borohydride aged for 48 hours at pH 13.7 contains more H_2 than freshly prepared hydride. As expected, the reaction with "old" sodium borohydride solution exhibits first-order rather than zero-order kinetics (gray in Figure 4b). We propose that the reduction at the catalytic interface follows the Langmuir–Hinshelwood mechanism (Scheme 1) and involves 4-NTP and adsorbed atomic hydrogen (Pt–H). Thus the reducers (H_2 and/or hydride) must penetrate the 4-NTP molecular layer and form Pt–H on the metal surface. The differences at different pH values can be attributed to the

Pt–H formation [see Eqs. (4)–(6)] in the presence of different reducers (H_2 or hydride):

$$H_2 + 2\,Pt \rightarrow 2\,Pt{-}H \quad (4)$$

$$BH_4^- + H_2O + 2\,Pt \rightarrow BH_3OH^- + 2\,Pt{-}H \quad (5)$$

$$R{-}NO_2 + 6\,Pt{-}H \rightarrow R{-}NH_2 + 6\,Pt + 2\,H_2O \quad (6)$$

The zero-order kinetics when hydride is the reducer is due to the low Pt–H concentration which makes the reaction rate independent from the 4-NTP concentration.

To further corroborate the hypothesis that the reduction at pH > 13 proceeds through a different reducer (hydride), SERS monitoring of the reaction at pH 14 is performed at different temperatures. Figure 5 reveals zero-order kinetics of

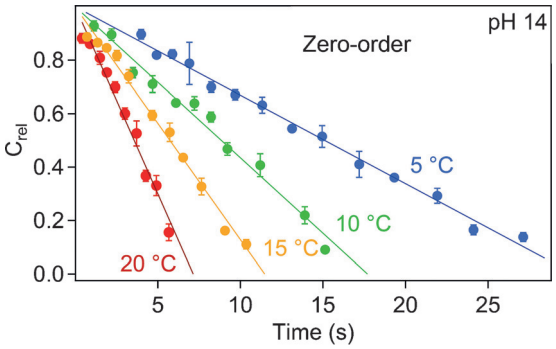

Figure 5. Temperature-dependent kinetic SERS monitoring of the catalytic reduction of 4-NTP in aqueous solution of sodium borohydride at pH 14. The relative contributions of 4-NTP are plotted at different reaction times. The reaction follows zero-order kinetics.

the reaction at all temperatures from 5 to 20 °C. The corresponding activation energy (see Figure S8) of this zero-order reduction is 64.5 kJ mol^{-1}, which is higher than the activation energy of the first-order reduction by H_2 (56.1 kJ mol^{-1}). We attribute this to the higher concentration of Pt–H in the case of H_2, which leads to a higher apparent rate constant $k_{app} = k_3[Pt{-}H]$ (see the discussion in the Supporting Information).

In summary, the pH-dependent catalytic reduction of 4-NTP in aqueous solution of sodium borohydride is studied by SERS. By using a temperature-controlled microfluidic reactor with high temporal resolution, the rate constants of the fast (few seconds) metal NP-catalyzed reaction are determined at different pH values and temperatures. At very basic conditions (pH > 13), the reaction exhibits zero-order kinetics. Under these conditions, sodium borohydride is stable in water and the formation of the competing reducer H_2 through hydride hydrolysis is not observed. We therefore conclude that the zero-order kinetics resembles the actual reduction by hydride. In contrast, below pH 13 (first-order kinetics), the reaction is dominated by the reduction with H_2, where the formation of the surface-adsorbed atomic hydrogen (Pt–H) is easier than in the sodium borohydride solution without H_2 (pH > 13). This competition has been overlooked so far since the reaction product 4-ATP for the two reducers is the same. Although the pH window of the borohydride reduction is very limited, one can slow down the hydrolysis process for a "real" hydride reduction by reducing the proton concentration, for example, in an aprotic environment.

Acknowledgements

This work was supported by the German Research Foundation (grant number XI 123/1-1). We thank B. Walkenfort for FEM simulations and nanoparticle characterizations. We also thank the reviewers for very fruitful comments. Financial and technical support by the University of Duisburg-Essen including CENIDE and NETZ is acknowledged.

Keywords: heterogeneous catalysis · microreactors · pH dependence · Raman spectroscopy · reduction

How to cite: *Angew. Chem. Int. Ed.* **2016**, *55*, 13729–13733
Angew. Chem. **2016**, *128*, 13933–13937

[1] a) H. C. Brown, *Boranes in Organic Chemistry*, Cornell University Press, Ithaca, **1972**; b) M. Periasamy, M. Thirumalaikumar, *J. Organomet. Chem.* **2000**, *609*, 137–151; c) T. Kawamoto, I. Ryu, *Org. Biomol. Chem.* **2014**, *12*, 9733–9742.

[2] H. I. Schlesinger, H. C. Brown, B. Abraham, A. C. Bond, N. Davidson, A. E. Finholt, J. R. Gilbreath, H. Hoekstra, L. Horvitz, E. K. Hyde, J. J. Katz, J. Knight, R. A. Lad, D. L. Mayfield, L. Rapp, D. M. Ritter, A. M. Schwartz, I. Sheft, L. D. Tuck, A. O. Walker, *J. Am. Chem. Soc.* **1953**, *75*, 186–190.

[3] H. I. Schlesinger, H. C. Brown, A. E. Finholt, J. R. Gilbreath, H. R. Hoekstra, E. K. Hyde, *J. Am. Chem. Soc.* **1953**, *75*, 215–219.

[4] a) P. A. Dub, T. Ikariya, *ACS Catal.* **2012**, *2*, 1718–1741; b) P. G. Andersson, I. J. Munslow, *Modern Reduction Methods*, Wiley-VCH, Weinheim, **2008**.

[5] W. Xie, C. Herrmann, K. Kömpe, M. Haase, S. Schlücker, *J. Am. Chem. Soc.* **2011**, *133*, 19302–19305.

[6] a) K. N. Heck, B. G. Janesko, G. E. Scuseria, N. J. Halas, M. S. Wong, *J. Am. Chem. Soc.* **2008**, *130*, 16592–16600; b) W. Xie, S. Schlücker, *Rep. Prog. Phys.* **2014**, *77*, 116502.

[7] a) P. L. Stiles, J. A. Dieringer, N. C. Shah, R. P. Van Duyne, *Annu. Rev. Anal. Chem.* **2008**, *1*, 601–626; b) S. Schlücker, *Angew. Chem. Int. Ed.* **2014**, *53*, 4756–4795; *Angew. Chem.* **2014**, *126*, 4852–4894; c) K. Kneipp, Y. Wang, H. Kneipp, L. T. Perelman, I. Itzkan, R. R. Da-sari, M. S. Feld, *Phys. Rev. Lett.* **1997**, *78*, 1667–1670; d) E. C. Le Ru, P. G. Etchegoin, *Annu. Rev. Phys. Chem.* **2012**, *63*, 65–87; e) Z. Q. Tian, B. Ren, *Annu. Rev. Phys. Chem.* **2004**, *55*, 197–229.

[8] a) V. Joseph, C. Engelbrekt, J. D. Zhang, U. Gernert, J. Ulstrup, J. Kneipp, *Angew. Chem. Int. Ed.* **2012**, *51*, 7592–7595; *Angew. Chem.* **2012**, *124*, 7712–7716; b) W. Xie, B. Walkenfort, S. Schlücker, *J. Am. Chem. Soc.* **2013**, *135*, 1657–1660; c) Q. L. Cui, G. Z. Shen, X. H. Yan, L. D. Li, H. Möhwald, M. Bargheer, *ACS Appl. Mater. Interfaces* **2014**, *6*, 17075–17081; d) J. M. Li, J. Y. Liu, Y. Yang, D. Qin, *J. Am. Chem. Soc.* **2015**, *137*, 7039–7042; e) W. Xie, S. Schlücker, *Nat. Commun.* **2015**, *6*, 7570.

[9] J. F. Huang, Y. H. Zhu, M. Lin, Q. X. Wang, L. Zhao, Y. Yang, K. X. Yao, Y. Han, *J. Am. Chem. Soc.* **2013**, *135*, 8552–8561.

[10] a) Y. F. Huang, H. P. Zhu, G. K. Liu, D. Y. Wu, B. Ren, Z. Q. Tian, *J. Am. Chem. Soc.* **2010**, *132*, 9244–9246; b) E. M. van Schrojenstein Lantman, T. Deckert-Gaudig, A. J. G. Mank, V. Deckert, B. M. Weckhuysen, *Nat. Nanotechnol.* **2012**, *7*, 583–

586; c) E. M. van Schrojenstein Lantman, O. L. J. Gijzeman, A. J. G. Mank, B. M. Weckhuysen, *ChemCatChem* **2014**, *6*, 3342 – 3346.
[11] a) G. Cristobal, L. Arbouet, F. Sarrazin, D. Talaga, J. Bruneel, M. Joanicot, L. Servant, *Lab Chip* **2006**, *6*, 1140 – 1146; b) K. R. Ackermann, T. Henkel, J. Popp, *ChemPhysChem* **2007**, *8*, 2665 – 2670; c) X. L. Zhang, H. B. Yin, J. M. Cooper, S. J. Haswell, *Anal. Bioanal. Chem.* **2008**, *390*, 833 – 840.
[12] K. N. Mochalov, V. S. Khain, G. G. Gil'manshin, *Kinet. Catal.* **1965**, *6*, 541 – 544.
[13] a) R. Liu, J. F. Liu, Z. M. Zhang, L. Q. Zhang, J. F. Sun, M. T. Sun, G. B. Jiang, *J. Phys. Chem. Lett.* **2014**, *5*, 969 – 975; b) K. Zhang, J. J. Zhao, Y. X. Li, B. H. Liu, *Anal. Chem.* **2015**, *87*, 8702 – 8708; c) Q. F. Zhang, Y. D. Zhou, E. Villarreal, Y. Lin, S. L. Zhou, H. Wang, *Nano Lett.* **2015**, *15*, 4161 – 4169.

Received: June 15, 2016
Published online: September 30, 2016

